Enhancing the Export Capability of Renewable Energy Bases through Two-Stage Small Signal Stability-Constrained Optimal Dispatch

Chuanqing Pu

Paper ID: 168

Github: `https://github.com/BigdogManLuo`

College of Smart Energy, Shanghai Jiao Tong University, Shanghai, China

October 2025

Outline

Background

- Increasing renewable energy penetration (wind, PV) reshapes power systems.
- Renewable energy bases are developed in weak-grid regions with limited synchronous generation.
- High RES integration leads to complex dynamics such as sub-/super-synchronous oscillations.
- Small-signal synchronous stability becomes a critical concern.

Motivation and Key Challenges

Motivation:

- Improve renewable energy export capacity while maintaining small-signal stability.
- Utilize energy storage for coordinated stability enhancement.

Key Challenges:

1. How to quantitatively evaluate small-signal stability in renewable energy bases?
2. How to integrate stability constraints into operational dispatch models?
3. How to efficiently solve the resulting non-convex optimization problem?

System Description

- Renewable energy base with multiple grid-following converters (GFCs) connected to a weak grid.
- Each GFC represents a wind turbine or PV system with local control.
- Energy storage systems (ESS) are co-located for flexibility and stability support.

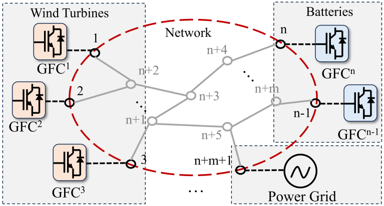

Figure: Schematic diagram of renewable energy base system.

Grid-Following Converter Model

The small-signal model of each GFC in the dq-frame is given by:

$$\boldsymbol{Y}_{GFC,i}(s) = \begin{bmatrix} Y_{dd,i}(s) & Y_{dq,i}(s) \\ Y_{qd,i}(s) & Y_{qq,i}(s) \end{bmatrix} \tag{1}$$

where:

$$Y_{dd,i}(s) = \frac{1}{L_f}\left(1 + \frac{k_{pc}k_{pp}}{L_f C_f s + k_{ic}k_{pp} + k_{pc}}\right), \tag{2}$$

$$Y_{dq,i}(s) = -\frac{1}{L_f}\left(\frac{k_{pc}k_{ip}}{L_f C_f s^2 + (k_{ic}k_{pp} + k_{pc})s + k_{ic}k_{ip}}\right), \tag{3}$$

$$Y_{qd,i}(s) = \frac{1}{L_f}\left(\frac{k_{pc}k_{ip}}{L_f C_f s^2 + (k_{ic}k_{pp} + k_{pc})s + k_{ic}k_{ip}}\right), \tag{4}$$

$$Y_{qq,i}(s) = \frac{1}{L_f}\left(1 + \frac{k_{pc}k_{pp}}{L_f C_f s + k_{ic}k_{pp} + k_{pc}}\right). \tag{5}$$

Parameters:

- L_f, C_f: Filter inductance and capacitance.
- k_{pc}, k_{ic}: Proportional/integral gains of current loop.
- k_{pp}, k_{ip}: Proportional/integral gains of power loop.
- C_f: Output filter capacitor.
- P_{GFC_i}: Steady-state injected power of ith GFC.

Network Susceptance Matrix

The susceptance matrix $\boldsymbol{B}$ is derived from the reduced admittance:

$$\boldsymbol{B} = \frac{1}{\omega_0} \operatorname{Im}(\boldsymbol{Y}_{red}), \tag{6}$$

$$\boldsymbol{B}_{\text{red}} = \boldsymbol{B}_{nn} - \boldsymbol{B}_{nm}\boldsymbol{B}_{mm}^{-1}\boldsymbol{B}_{mn}, \tag{7}$$

$$b_{ij} = \begin{cases} \sum_{j=0, j\neq i}^{n+m+1} \frac{1}{\omega_0 L_{ij}}, & j = i \\ -\frac{1}{\omega_0 L_{ij}}, & j \neq i \end{cases} \tag{8}$$

Parameters:

- L_{ij}: line inductance between nodes i and j.
- Submatrices $\boldsymbol{B}_{nn}$, $\boldsymbol{B}_{nm}$, $\boldsymbol{B}_{mn}$ represent coupling between GFC and passive nodes.

Characteristic Equation and Homogeneous System

The overall small-signal stability is governed by:

$$\det\left[\mathrm{diag}(Y_{GFC1}(s), \ldots, Y_{GFCi}(s)) + \boldsymbol{B} \otimes \gamma(s)\right] = 0. \tag{9}$$

Under heterogeneous converter parameters, the system can be represented equivalently by:

$$\det\{\boldsymbol{I}_n \otimes \boldsymbol{G}(s)\gamma^{-1}(s) + \boldsymbol{P}_G^{-1}\boldsymbol{B} \otimes \boldsymbol{I}_2\} = 0. \tag{10}$$

where:

$$\boldsymbol{G}(s) = \sum_{i=1}^{n} u_{i1} v_{i1} \boldsymbol{P}_G^{-1} \boldsymbol{Y}_{GFC,i}(s), \tag{11}$$

$$\boldsymbol{P}_G = \mathrm{diag}(P_{GFC_1}, \ldots, P_{GFC_i}). \tag{12}$$

Here u_{i1}, v_{i1} denote left/right eigenvector elements of $\boldsymbol{P}_G^{-1}\boldsymbol{B}$.

Decoupled Stability and Definition of gSCR

A homogeneous multiple-converter system (MCS) can be decomposed into n independent single-converter systems (SCS):

$$\prod_{i=1}^{n} \det\{\boldsymbol{G}(s)\gamma^{-1}(s) + \lambda_i \boldsymbol{I}_2\} = 0. \tag{13}$$

Thus, the system stability depends on eigenvalues λ_i of $\boldsymbol{P}_G^{-1}\boldsymbol{B}$. The minimal eigenvalue defines the generalized short-circuit ratio (gSCR):

$$gSCR = \min_{\lambda} \lambda\{\boldsymbol{P}_G^{-1}\boldsymbol{B}\}. \tag{14}$$

Physical Meaning:

- gSCR reflects coupling strength between inverter group and grid.
- Lower gSCR $\Rightarrow$ weaker grid, reduced damping margin.
- gSCR forms the basis for embedding small-signal stability as a convex constraint in the optimization model.

Objective and Decision Variables

$$\max_{\boldsymbol{z}^{(i)},\boldsymbol{z}^{(ii)}} F = \sum_t \pi_G \sum_i P_{Wi,t} - C_B \sum_j (P_{Bdch,j,t} - P_{Bch,j,t}) \quad (15)$$

Decision variables:

- $P_{Wi,t}$: Injected wind/PV power.
- $P_{Bdch,j,t}$, $P_{Bch,j,t}$: Battery discharge/charge power.

Constraints:

- Power limits, SOC bounds, transmission capacity.
- Small-signal stability constraint: $\boldsymbol{B} - S_{base}\beta_{CgSCR}\boldsymbol{P}_G \succeq 0$.

Parameters:

- π_G: On-grid power price.
- C_B: Battery operation cost.
- β_{CgSCR}: Critical gSCR threshold.
- S_{base}: Base power.

Two-Stage Dispatch Framework

1. **Day-ahead scheduling:** Optimize expected cost using day-ahead forecasts.
2. **Real-time adjustment:** Adjust renewable energy dispatch based on ultra-short-term forecasts to handle deviations.

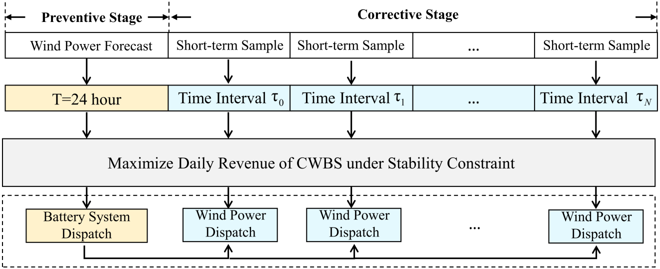

Figure: Two-stage renewable energy base operation framework.

System Topology

The case study uses a 7-bus renewable energy base with 3 wind farms and 1 battery system. The system topology is shown in the figure.

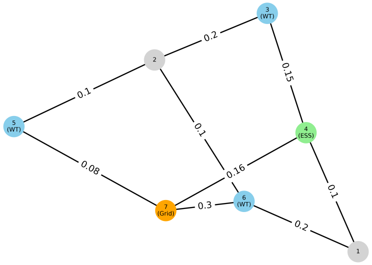

Figure: Topology of the 7-bus renewable energy base system. The wind farms WT1, WT2, and WT3 are connected to buses 3, 5, and 6, respectively, while the battery energy storage system ESS1 is connected to bus 4. The bus 7 is connected to the infinite grid.

Key Parameters

The parameters of the grid-followed converters and battery system are summarized below. **Key Parameters:**

Symbol	Description	Value
S_{base}	Base power (MVA)	1.5
L_f, C_f	Filter elements (p.u.)	0.05, 0.05
E_{max}	Max battery capacity (MWh)	7
P_{Bdch}^{max}	Max discharge (MW)	3.5
η_{dch}, η_{ch}	Efficiency	0.9, 0.9

Wind Power Forecast

The day-ahead and actual wind power forecasts for WT1 to WT3 are shown below.

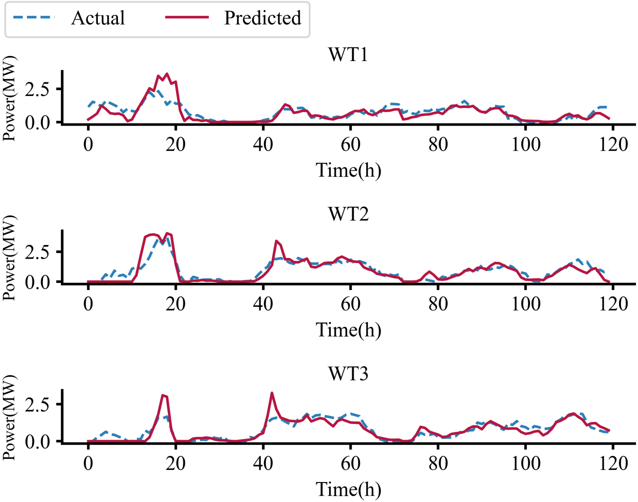

Optimal Dispatch Plan:

- The battery charging schedule aligns with periods of high wind power availability and reduced stability margins.
- Discharging occurs during low wind power availability to maintain stability and maximize export capacity.
- This coordinated strategy minimizes wind curtailment and enhances overall system efficiency.

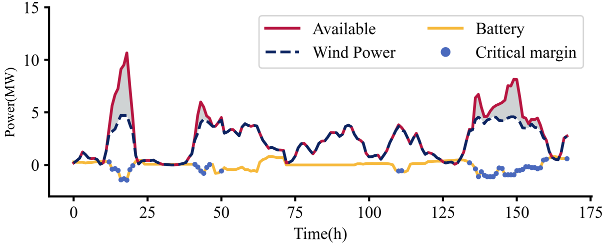

Figure: Optimal dispatch plan of wind turbines and battery system.

Comparison with Existing Methods

	Single-stage	Ref.	Proposed
Mean Revenue (CNY)	44622.28	45897.57	47689.74
Export Energy (MWh)	52.50	54.00	56.11
Curtailment	23.74%	22.21%	20.2%
Mean gSCR	13.60	13.54	11.96

Table: Performance comparison under stability constraints.

- The proposed two-stage strategy achieves the highest revenue, with a 7.79% improvement compared to the single-stage method.
- Export energy is maximized, reducing wind curtailment to 20.2%, the lowest among the compared methods.
- The mean gSCR is maintained above the critical threshold, ensuring system stability while enhancing operational efficiency.

Conclusions

- Proposed two-stage dispatch strategy integrates small-signal stability (gSCR) into optimization.
- SDP-based reformulation ensures tractable convex optimization.
- Achieves **7.79% improvement** in renewable export capacity.

Limitations and Future Work

- Real-world gSCR measurement uncertainty.
- Coordinated RES forecasting and dispatch to improve the export capacity. (https://ieeexplore.ieee.org/document/11069389)
- Extend to multi-energy hybrid systems (wind–PV–hydrogen).

Thank You!